Title: Enhanced cytosolic NADP-ME2 activity in *A. thaliana* affects plant development, stress tolerance and specific diurnal and nocturnal cellular processes

Author: Mariana B. Badia Cintia L. Arias Marcos A. Tronconi Verónica G. Maurino Carlos S. Andreo María F. Drincovich Mariel C.Gerrard Wheeler

PII: S0168-9452(15)30072-8
DOI: http://dx.doi.org/doi:10.1016/j.plantsci.2015.09.015
Reference: PSL 9294

To appear in: *Plant Science*

Received date: 7-6-2015
Revised date: 11-9-2015
Accepted date: 19-9-2015

Please cite this article as: Mariana B.Badia, Cintia L.Arias, Marcos A.Tronconi, Verónica G.Maurino, Carlos S.Andreo, María F.Drincovich, Mariel C.Gerrard Wheeler, Enhanced cytosolic NADP-ME2 activity in A.thaliana affects plant development, stress tolerance and specific diurnal and nocturnal cellular processes, Plant Science http://dx.doi.org/10.1016/j.plantsci.2015.09.015

Enhanced cytosolic NADP-ME2 activity in *A. thaliana* affects plant development, stress tolerance and specific diurnal and nocturnal cellular processes

Mariana B. Badia[1], Cintia L. Arias[1], Marcos A. Tronconi[1], Verónica G. Maurino[2], Carlos S. Andreo[1], María F. Drincovich[1], Mariel C. Gerrard Wheeler[1,*] gerrard@cefobi-conicet.gov.ar

[1]Centro de Estudios Fotosintéticos y Bioquímicos (CEFOBI), Universidad Nacional de Rosario, Suipacha 531, 2000 Rosario, Argentina.

[2]Institute of Developmental and Molecular Biology of Plants, Plant Molecular Physiology and Biotechnology Group, Heinrich-Heine-Universität, Universitätsstr. 1, and Cluster of Excellence on Plant Sciences (CEPLAS), 40225 Düsseldorf, Germany.

[*]Correspondence to: Suipacha 531, 2000 Rosario, Argentina. Tel.: 54 341 4371955; fax: 54 341 4370044.

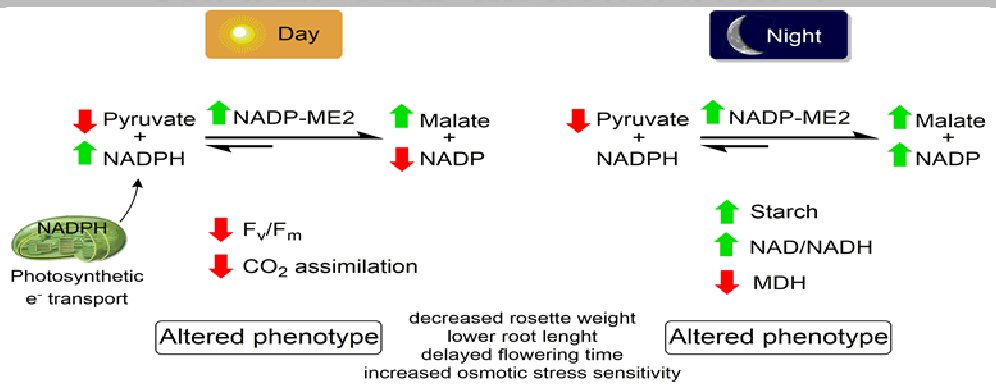

Graphical Abstract

Highlights

We characterized Arabidopsis plants over-expressing NADP-ME2 constitutively.
The transgenic plants exhibited increased sensitivity to osmotic stress conditions.
Primary metabolism and redox status were affected in the over-expressing lines.
These alterations indicate the relevance of NADP-ME2 in plant homeostasis.

Abstract

Arabidopsis thaliana has four NADP-dependent malic enzymes (NADP-ME 1-4) for reversible malate decarboxylation, with NADP-ME2 being the only cytosolic isoform ubiquitously expressed and responsible for most of the total activity. In this work, we further investigated its physiological function by characterizing Arabidopsis plants over-expressing NADP-ME2 constitutively. In comparison to wild type, these plants exhibited reduced rosette and root sizes, delayed flowering time and increased sensitivity to mannitol and polyethylene glycol. The increased NADP-ME2 activity led to a decreased expression of other ME and malate dehydrogenase isoforms and generated a redox imbalance with opposite characteristics depending on the time point of the day analyzed. The over-expressing plants also presented a higher content of C_4 organic acids and sugars under normal growth conditions. However, the accumulation of these metabolites in the over-expressing plants was substantially less pronounced after osmotic stress exposure compared to wild type. Also, a lower level of several amino acids and osmoprotector compounds was observed in transgenic plants. Thus, the gain of NADP-ME2 expression has profound consequences in the modulation of primary metabolism in *A. thaliana*, which reflect the relevance of this enzyme and its substrates and products in plant homeostasis.

Abbreviations

ADH, alcohol dehydrogenase; DAB, 3,3′-diaminobenzidine; DCPIP, 2,6-dichlorophenol indophenol; G3P, glyceraldehyde-3P; GABA, γ-aminobutyrate; GC-MS, gas chromatography followed by mass spectrometry; MDH, malate dehydrogenase; ME, malic enzyme; PEG, polyethylene glycol; PPDF, photosynthetic photon flux density; qRT-PCR, quantitative real time polymerase chain reaction.

Keywords: NADP-malic enzyme; osmotic stress; organic acids; plant homeostasis

1. Introduction

Organic acids have many different and essential functions in plant development and survival under fluctuating conditions. The level of organic acids accumulation and their chemical nature vary among species, developmental stages, organ and tissue types and environmental conditions [1]. Within the four carbon organic acids, the dicarboxylate malate plays important roles in all kind of plants as it is an universal tricarboxylic acid cycle intermediary [2]. It is also involved in defense responses [3], cellular pH regulation [4] and stomatal movement [5]. Recent studies indicated that it is an important storage and transport molecule of photosynthetically assimilated carbon even in C_3 plants [6,7], and a transcriptional regulator in metabolite signalling [8]. Malate also takes part in the specialized photosynthetic CO_2 concentrating mechanisms given in C_4 and CAM plants [9].

Arabidopsis thaliana is a fumarate/malate hyper-accumulator [2,10,11]. Malic enzyme (ME) is involved in malate metabolism as it catalyzes its oxidative decarboxylation generating pyruvate, CO_2 and reducing power as NADH or NADPH [9]. The C_3 dicot Arabidopsis possesses four NADP-dependent isoforms and two that prefer NAD as cofactor (NADP-ME1-4 and NAD-ME1-2) [12,13]. The different family members have distinct subcellular localization and a particular tissular and developmental expression pattern [12-14]. The biochemical characterization of the recombinant proteins revealed that they differ in their structural and kinetic properties; e.g., native structure, mechanism of catalysis, kinetic parameters and metabolic regulation effectors [14-20]. Besides having decarboxylating activity, the NADP-ME isoforms also catalyze the reverse reaction (reductive carboxylation of pyruvate) with high performance, suggesting that both reactions may occur in vivo in Arabidopsis [15,20]. By contrast, its NAD-dependent counterparts are active only in the oxidation of malate [17]. The divergent properties of these isoforms suggest non-redundant roles unique to each family member in plant metabolism [21].

NADP-ME2 (TAIR: AT5G11670; EC 1.1.1.40) is the only cytosolic isoform found in all Arabidopsis organs and it is responsible for the majority of the activity measured in mature plant tissues. The expression of other cytosolic proteins (NADP-ME1 and NADP-ME3) is limited to cell-specific or plant growth signals. In adult plants, NADP-ME1 is localized in the vascular cylinder of some secondary roots, while NADP-ME3 is present mainly in trichomes and pollen [12,14]. NADP-ME2 is active as a homotetramer constituted by monomers of 65 kDa [21]. Recent studies showed that the lack of an active NADP-ME2 in T-DNA insertional mutants results in altered metabolic profiles [22,23]. NADP-ME2 is functional in the veins of *A. thaliana*, where it would be relevant to sugar metabolism [22]. Moreover, it is involved in the production of reactive oxygen species during the early plant basal defense against hemibiotrophic fungal pathogens [23]. It could also participate in other responses, as NADP-ME2 transcript accumulated in response to both intra- and extracellular oxidative stress source [24]. In this regard, the over-expression of a cytosolic NADP-ME of rice in *A. thaliana* gives osmotic and salt stress tolerance [25,26], although the specific role this enzyme fulfills has not been elucidated.

In this work a comprehensive characterization in terms of physiology and phenotype of Arabidopsis plants with increased NADP-ME2 expression is presented. These plants showed an altered content of redox compounds, organic acids, sugars and other key metabolites. In addition, the over-expressing plants presented an anomalous phenotype and a higher sensitivity to osmotic stress treatments. The metabolic and phenotypic changes caused by the gain of NADP-ME2 activity were different from those observed in Arabidopsis lines over-expressing the plastidic maize NADP-ME involved in C_4 photosynthesis [6,7]. This suggests an isoform-dependent response and/or a differential effect depending on the interfered malate pathways in the different subcellular compartments.

2. Material and methods

2.1 Plant lines and growing conditions

NADP-ME2 over-expressing *A. thaliana* Columbia-0 lines were obtained by transforming wild type plants with a construct carrying the NADP-ME2 cDNA under regulation of the constitutive 35SCaMV promoter [23]. A modified version of the binary vector pGreenII containing the BASTA resistance gene was used [6]. Three non-segregating T3 independent transgenic lines were analyzed: 7.11, 4.20 and 6.20. These lines were selected taking into consideration their increase in NADP-ME activity (nearly 10 fold relative to the wild type) and differ from those in [23], which showed only 2.5-4 fold increase in NADP-ME activity relative to wild type plants.

After 72 hours at 4°C in the dark to achieve a synchronized germination, the plants were grown in soil in a chamber with a 16:8 h light:dark regimen at 25°C and a photosynthetic photon flux density (PPDF) of 100 $\mu E\ m^{-2}\ s^{-1}$. Samples of rosette leaves were collected 32 days after sowing at different times of the day-night period, frozen in liquid N_2 and stored at -80°C. For osmotic stress assays, plants were subjected to irrigation with 15% (w/v) polyethylene glycol (PEG) 6000, 100 mM NaCl, water (control plants), or maintained without irrigation for drought treatment from day 32 [25]. For root length and germination percentage determinations, the plant growth was performed in plates with 1X MS medium

[27] containing 0.6% (w/v) phytagel. For osmotic stress treatment, NaCl (30-100 mM) or mannitol (100-250 mM) was added to the MS medium. Previously, seeds were sterilized with 0.5% (v/v) Triton X-100 and 50% (v/v) ethanol for 3 minutes, washed with 95% (v/v) ethanol and dried on filter paper.

2.2 Quantification of pigments

Samples of rosette leaves were homogenized in a mortar and suspended in 3 ml of 96% (v/v) ethanol per 50 mg of tissue. After incubation for 1 hour in the dark, the extracts were centrifuged for 5 minutes at 10,000 x g and the supernatants used to measured absorbance at 665, 649 and 480 nm. The concentrations of chlorophyll a, chlorophyll b and carotenoids were obtained according to [28].

2.3 Gas exchange and chlorophyll fluorescence analysis

CO_2 exchange was determined with an infrared gas analyzer (Qubit Systems). Detached leaves were sealed in a compartment with a PPDF of 100 μE m^{-2} s^{-1} provided by a LED lamp, at 25°C. Chlorophyll fluorescence was measured using a package from Qubit Systems. Initially, plant material was incubated in the dark for 30 minutes. Basal (F_0) and maximum (F_m) fluorescence were measured with very weak red light or saturating white light pulse (5000 μE m^{-2} s^{-1}), respectively. Quantum yield of photosynthesis (F_v/F_m) was determined as $(F_m–F_0)/F_m$.

2.4 Preparation of protein extracts

Samples of rosette leaves were homogenized in mortars with liquid N_2 and suspended in extraction buffer (100 mM Tris-HCl pH 7.5, 2 mM EDTA, 5 mM $MgCl_2$, 10 mM 2-mercaptoethanol, 10% (v/v) glycerol, 1% (v/v) protease inhibitor cocktail (Sigma) and 0.5% (v/v) Triton X-100) using 0.2 ml per 100 mg of fresh weight. The homogenate was centrifuged at 12,000 x g for 15 minutes at 4°C. Then, the supernatant was used for protein concentration and activity assays, or was prepared for electrophoresis.

2.5 Enzyme activity and protein concentration assays

Protein concentration was determined by the BioRad protein assay using total serum protein as standard. Activity assays were performed at 30ºC in a Helios β Unicam spectrophotometer in a volume of 0.5 ml, following the production or consumption of NAD(P)H at 340 nm (ε_{340nm}=6.22 mM^{-1} cm^{-1}).

NADP-ME activity was assayed using a mixture of 50 mM Tris-HCl pH 7.5, 0.5 mM NADP, 10 mM malate, 10 mM $MgCl_2$ and 10 μl of extract containing the enzyme [12]. NAD-ME activity was determined in a medium with 50 mM MES-NaOH pH 6.6, 10 mM $MnCl_2$, 2 mM NAD, 10 mM malate and 1 U of malate dehydrogenase (MDH; Sigma). Once the MDH catalyzed reaction reached equilibrium, 20 μl of extract containing the enzyme were added. As NAD-ME and MDH reactions compete for the same substrates, the addition of exogenous MDH ensures that malate is consumed by the NAD-ME reaction [13]. NAD-MDH activity was determined in a medium containing 50 mM Tris-HCl pH 7.2, 0.2 mM NADH, 2 mM oxaloacetate, 0.02% (v/v) Triton X-100 and 0.5 μl of extract containing the enzyme [29]. NADP-MDH initial activity was assayed using a reaction mixture containing 25 mM Tricine-KOH pH 8.3, 1 mM EDTA, 150 mM KCl, 0.2 mM NADPH, 2 mM oxaloacetate, 5 mM DTT and 10 μl of extract containing the enzyme. In addition, NADP-MDH total activity was determined after incubating the protein extract with 100 mM DTT [29].

2.6 Gel electrophoresis

Native PAGE was performed using 6% (w/v) polyacrylamide gels. Then, the proteins were assayed for NADP-ME activity by incubation in a solution of 50 mM Tris-HCl pH 7.5, 10 mM malate, 0.5 mM NADP, 10 mM $MgCl_2$, 35 μg ml^{-1} nitroblue tetrazolium and 0.85 μg ml^{-1} phenazine methosulfate at 30ºC.

2.7 Real time polymerase chain reaction (*qRT-PCR)*

Relative gene expression analysis was carried out by qRT-PCR on a Mx3000P QPCR system using the MxPro QPCR software version 4.10 (Stratagene). Total RNA was extracted from 100 mg of rosette leaves with the Trizol reagent (Invitrogen) and treated with RQ1 DNase (Promega). The concentration and purity of the preparations were determined spectrophotometrically and the integrity was assayed by agarose 1% (w/v) gel electrophoresis. Four micrograms of RNA were reverse transcribed with 200 U of SuperScriptII (Invitrogen) using oligodT as primer. Four-fold dilutions of the cDNAs synthesized were used as template for quantitative PCR assays. The PCR mix contained the dye SYBRGreen I (Invitrogen) as reporter of fluorescence, 3 mM $MgCl_2$, 0.25 μM of each primer, 0.2 mM dNTP and 0.025 U Platinum DNA polymerase in the presence of the buffer provided by the supplier (Invitrogen). The oligonucleotide specific primers pairs used are listed in Supplementary Table 1.

Thermal cycling settings were as follows: 2 minutes at 94°C for initial denaturation; 46 cycles at 96°C for 10 seconds, 56°C for 15 seconds and 72°C for 20 seconds for amplification; and 72°C for 10 minutes for final elongation. Melting curves for each reaction were determined by increasing the temperature from 65°C to 98°C. The PCR specificity was verified by melting curve and gel electrophoresis analysis of the PCR products. Then, relative gene expression was determined using a modified version of the comparative $2^{-\Delta\Delta CT}$ method [30] and polyubiquitin 10 (AT4G05320) as normalizing gene [31]. Efficiencies and error propagation were calculated according to [32,33]. Each sample was run in triplicate and determined in at least two biological replicas.

2.8 Determination of pyridine nucleotides

Samples of rosette leaves were homogenized in mortars with liquid N_2 and suspended in 0.2 N HCl for extraction of NAD(P) or 0.2 M NaOH for extraction of NAD(P)H [34]. After centrifuging for 10 minutes at 16,000 x g at 4°C, each supernatant was boiled for 1 minute, cooled and neutralized. Determinations were performed spectrophotometrically at 30°C, following the decrease of absorbance at 600 nm caused by the reduction of 2,6-dichlorophenol indophenol (DCPIP) in a volume of 0.5 ml. The assay medium for NAD(H) determination contained 200 mM Tricine pH 7.5, 10 mM $MgCl_2$, 2 mM EDTA, 0.12 mM DCPIP, 1 mM PMS, 3U of alcohol dehydrogenase (ADH; Sigma) and 50 µl of extract. The addition of 15 µl of absolute ethanol initiated the reaction. The assay medium for NADP(H) determination contained 2 mM glucose-6-P instead of ADH. In this case, the reaction was initiated with 2 U of yeast glucose-6-P dehydrogenase (Sigma). Calibration curves were constructed using standard solutions of NAD and NADP.

2.9 Diaminobenzidine stain for hydrogen peroxide

Twenty-day-old leaves were immersed for 8 hours in 1 mg/ml 3,3´-diaminobenzidine (DAB) solution. Then, the samples were destained by soaking in 100% ethanol for 3 hours and examinated under a microscope. The presence of hydrogen peroxide causes polymerization of DAB, yielding a brown color [35].

2.10 Quantification of sugars and organic acids by enzymatic methods

Samples of rosette leaves (100 mg) were homogenized in a mortar with liquid N_2 and suspended in 1.4 ml methanol. The extracts were then incubated for 15 minutes at 70°C. After addition of 0.75 ml of chloroform, the extracts were incubated for 5 minutes at 37°C, diluted with 1.5 ml of distilled water and centrifuged at 2,200 x g for 15 minutes. The polar phase was aliquoted, dried down and dissolved in water. The glucose, fructose, sucrose, malate, fumarate and pyruvate contents were determined by enzymatic endpoint assays according to [36,37]. For starch determination, the methanol-insoluble phase was homogenized in 0.2 N KOH, adjusted to pH 5.5 using 1 N acetic acid and digested with 2.5 U amyloglucosidase and 3.5 U α-amylase by overnight incubation at 25°C. The digestion was incubated at 95°C for 5 minutes and centrifuged for 10 minutes at 16,000 x g. The glucose content of the resulting supernatant was determined as described above. Calibration curves were constructed using standard solutions of each metabolite tested.

2.11 Metabolite level determination by gas chromatography followed by mass spectrometry (GC-MS)

Metabolite analysis by GC-MS was carried out essentially as described in [38]. Polar metabolites were extracted as described in section 2.10 plus the addition of 15 µg ribitol. Dried samples were then derivatized by methoxyamination using a 20 mg/ml solution of methoxyamine hydrochloride in pyridine, and treated with N-Methyl-N-(trimethylsilyl)trifluoroacetamide for subsequent trimethylsilylation. After each addition, incubations of 90 and 30 minutes at 37°C were performed, respectively. An aliquot of the derivatized sample was injected at 230ºC with helium as carrier gas and a flow rate set to 1 ml $minute^{-1}$ into a Shimadzu QP 2010 plus GC-MS system equipped with a VF-5ms column (30 m x 0.25 mm, Varian). Injection was done in split mode with the split ratio adjusted to 1:25. The GC program used was as follows: 5 minutes at 70ºC, followed by a 5ºC per minute ramp to 350ºC, and holding at this temperature for 5 minutes. The ion source and interface temperatures were 200ºC and 250ºC, respectively. Ions were generated by a 70 eV electron beam and two scans per second were registered in the mass range 50-600 m/z. Mass spectra and chromatograms were processed using the Automatic Mass Spectral Deconvolution and Identification System (http://chemdata.nist.gov/mass-spc/amdis/). The compound identification was performed by comparing mass spectra with those in the Golm Metabolome Database [39]. The minimum match factor of the metabolites reported was 85. Signals were normalized using ribitol as internal standard molecule, allowing a relative metabolite quantification [6,23,38]. Each sample was run in duplicate and repeated in three independent biological replicas.

2.12 Statistical analysis

Significance was determined by the Student's t test ($p < 0.05$) using the SigmaPlot software. The sample size is indicated in each figure or table.

3. Results and Discussion

3.1 Molecular and physiological characterization of A. thaliana NADP-ME2 over-expressing plants

Arabidopsis NADP-ME2 over-expressing plants (lines 7.11, 4.20 and 6.20) were obtained from independent transformation events. When grown in long days under standard light, temperature and humidity conditions, these transgenic plants were smaller than wild type (Figure 1a). The transgenic plants exhibited lower root length and rosette weight and a delayed flowering time relative to wild type (Figures 1b to 1d). No significant differences were found in the other phenotypic parameters analyzed such as silique and seed number and rate of germination (Figures 1e to 1g). In addition, chlorophyll and carotenoid contents were similar to wild type (Figures 1h to 1j). Net rate of CO_2 assimilation and F_v/F_m ratio were significantly lower in the transgenic plants (Figures 1k and 1l). In turn, the content of starch measured at different times of the day-night cycle was higher in the over-expressing plants (data for the ending of the day are shown in Figure 1m).

Total NADP-ME activity in leaf protein extracts of the over-expressing plants was examined. The line 7.11 showed ~9 fold increase of NADP-ME activity relative to the wild type (Figure 2a); while lines 4.20 and 6.20 presented an increase of ~12 and ~7 times, respectively, compared to wild type (Supplementary Figure 2). This increment was dependent on the time of sampling, being even higher (~2 fold) towards the end of the night (Figure 2; Supplementary Figure 2). Consistent with this, we observed an increment of a protein band stained for NADP-ME activity at ~440 kDa (Figure 2a). This band may correspond to NADP-ME2 (endogenous and over-expressed), as the other NADP-ME isoform usually found in leaves is plastidic NADP-ME4, which is displayed as two bands with NADP-ME activity at ~260 and ~130 kDa [12]. Thus, *A. thaliana* NADP-ME2 over-expressing plants showed increased NADP-ME2 activity and the protein synthesized from the transgene had a similar native conformation to that of the endogenous enzyme.

The relative expression level of NADP-ME2 was ~24 times higher in line 7.11 in comparison to the wild type, as assessed by qRT-PCR (Table 1). Similar transcript levels were found at both the end of day and night, in accordance with the constitutive promoter used to generate the over-expressing plants. In wild type plants, NADP-ME2 gene expression did also not change during a day-night cycle (expression ratio end of the day/end of the night = 1.3). Thus, the differences in NADP-ME activity measured in the transgenic plants by the ending of the day and night (Figure 2a) could be due to translational or posttranslational control [20,40,41].

3.2 Modulation of the expression and activity of other enzymes acting on malate in NADP-ME2 over-expressing plants

We analyzed if the expression level of other enzymes acting on malate was affected in the NADP-ME2 over-expressing plants. We found that the relative expression level of NADP-ME4 by the end of the night was decreased in the NADP-ME2 over-expressing plants in comparison to the wild type (Table 1). A parallel reduction of the transcripts was observed for NAD-ME1 and NAD-ME2 at night (Table 1). By the ending of the light period, we measured a slight increment of the NAD-ME1 relative expression in the transgenic plants (Table 1). This higher expression level of one of the NAD-ME genes could explain the higher total NAD-ME activity found in the transgenic plants, at least at the end of the day (Figure 2b). NAD-ME activity may also be regulated by translational or post-translational mechanisms. Furthermore, we cannot rule out that the enhanced NAD-ME activity could be due to the NAD-ME activity of NADP-ME2, as this enzyme can also use NAD as cofactor in vitro, although with lower affinity [15].

The activity pattern of malate dehydrogenase (MDH), another enzyme involved in malate metabolism, was analyzed. MDH catalyzes the reversible conversion of malate to oxaloacetate concomitant with the reduction of NAD(P). Total NAD-MDH activity of leaf crude extracts from NADP-ME2 transgenic plants was lower than in wild type plant, at both the end of the day and night (Figure 2c; Supplementary Figure 2). The NADP-MDH activity was similar in both types of plants (Figure 2d). The Arabidopsis genome has eight genes encoding NAD-MDH isoforms and a single gene for a NADP-MDH. These genes encode products with different subcellular location and physiological functions [42-47]. Analysis of the transcript level of these isoforms in NADP-ME2 over-expressing plants indicated a reduction of the expression of most of them by the ending of the night, while no differences were observed by the ending of the day (Table 1). Again, translational or post-translational mechanisms may be operating, and would explain the differences between the results of qRT-PCR (Table 1) and activity assays (Figures 2c and d).

Overall, NADP-ME2 over-expression led to altered expression and activity of related enzymes, already located in the same compartment as NADP-ME2, the cytosol, or in other cell organelles.

3.3 Pyridine nucleotide pool sizes and hydrogen peroxide stain in NADP-ME2 over-expressing plants

Since NADP-ME reaction involves the conversion of NADP to NADPH, the content of these nucleotides was determined. Under normal conditions, the NADP/NADPH ratio was lower in the transgenic plants compared to the wild type at the ending of the light period, while it was higher at night (Figure 2e; Supplementary Figure 2). These differences were due mainly to a decrease of the NADP diurnal pool and an increased content of nocturnal NADP in the over-expressing plants.

A similar light-dependent pattern was observed for the NAD/NADH ratio (Figure 2f; Supplementary Figure 2). By the end of the day, the NADP-ME2 transgenic plants presented lower NAD and higher NADH levels than the wild type. Conversely, the transgenic plants showed an increase of NAD and a decrease of its reduced form by the end of the night (Figure 2f; Supplementary Figure 2).

Besides the natural potential of NADP-ME2 to generate changes in the redox state of pyridine nucleotides, it is also possible that perturbations in their processes of synthesis and/or degradation are occurring due to the higher levels of Arabidopsis NADP-ME2 activity in the transgenic plants.

In addition, leaves of transgenic plants showed higher DAB stain for hydrogen peroxide than the wild type (Figure 2g), which may be linked to the observed redox balance disturbance.

3.4 Metabolite profiles in NADP-ME2 over-expressing plants

Several polar metabolites were measured through enzymatic endpoint and GC-MS methods (Figure 3 and Table 2) in order to identify disturbances caused by the increased NADP-ME2 activity. We found that NADP-ME2 over-expressing plants had higher malate and fumarate content than the wild type, especially towards the ending of the day (Figure 3; Supplementary Figure 3). Glucose and fructose levels increased, particularly towards the end of the night, while sucrose remained unchanged in all genotypes (Figure 3; Supplementary Figure 3). On the other hand, the content of pyruvate, the product of the NADP-ME direct reaction, was lower in the transgenic plants by the end of both periods (Figure 3; Supplementary Figure 3).

Changes in the relative amount of other metabolites were also observed in the NADP-ME2 over-expressing plants in comparison to the wild type (Table 2). Oxalate, maleate, glyceraldehyde-3P (G3P) and maltose showed a significant increment in the transgenic plants regardless of the moment of the day analyzed (Table 2). On the other hand, succinate and citrate raised in the transgenic plants only during the day; while lactate, several amino acids, urea, galactinol and trehalose were increased specifically during the night (Table 2).

Overall, it is clear that the gain of NADP-ME2 activity makes a great impact on the primary metabolism of Arabidopsis. This metabolic disturbance not only includes modifications in organic acid levels, but also changes in sugar and nitrogen-containing compound accumulation. Furthermore, the repercussion of the artificial enhance of NADP-ME2 activity appears to be time-of-day-dependent.

3.5 Response of NADP-ME2 over-expressing plants to osmotic stress treatments

As *A. thaliana* over-expressing a rice cytosolic NADP-ME showed high salt and osmotic stress tolerance [25,26], NADP-ME2 over-expressing plants were subjected to different osmotic stress conditions to evaluate their response. To affect plant water potential, NADP-ME2 transgenic and wild type plants were watered with 100 mM NaCl, 15% (w/v) PEG 6000 or held without irrigation. After 14 days, the NADP-ME2 over-expressing plants were significantly more sensitive to the PEG treatment than wild type (Figures 4a and 4b). This differential behavior was not observed for salt or drought stress in the conditions tested (Figure 4b). In addition, the exposure to a high mannitol concentration (250 mM) significantly reduced the germination rate of the transgenic plants (Figure 4c).

Given that the NADP-ME2 over-expressing plants showed a reduction of PEG tolerance, we analyzed the new redox and metabolic status reached in leaves of plants after 48 hours of PEG irrigation using samples taken at the middle of the day. We observed that the contents of NADP, NADPH and NAD after treatment were enhanced in wild type plants, while the levels of NADP, NAD and NADH were increased in the transgenic plants (Figure 4d). Generally, plants under stress have a higher demand of NADPH, which is required for detoxification and signaling processes [48]. The fact that NADPH levels did not increase in the NADP-ME2 transgenic plants in response to PEG treatment suggest that the over-expressing plants cannot afford the maintenance of levels and ample supply of NADPH, which are critical for cell survival.

In addition, changes in the content of polar metabolites triggered by PEG treatment were significantly different when comparing NADP-ME2 over-expressing and wild type plants. An increase of malate, fumarate, pyruvate, glucose, fructose and sucrose was observed in the wild type (Figure 4e).

Water deficiency frequently increases carbon concentration in plant organs [49]. However, this increase did not occur in the transgenic plants (Figure 4e). We also observed a PEG-induced increment in the content of a larger number of metabolites in wild type plants compared to NADP-ME2 over-expressing plants, including organic acids, amino acids, several carbohydrates and sugar alcohols (Table 3). The most prominent changes were in the accumulation of alanine, valine, γ-aminobutyrate (GABA), melibiose and raffinose. However, these increases could not be sustained in equal levels in the over-expressing plants, probably due to a defect in the synthesis or an enhanced degradation of these compounds, linked to the altered metabolic state observed in these plants even under non-stress conditions (Figures 2 and 3, Table 2). Some of the compounds mentioned above stabilize macromolecules and biological structures and contribute to an osmotic adjustment in order to allow continuous water absorption and plant swelling [50]. Among them, galactinol and raffinose belong to a family of oligosaccharides acting as osmoprotectors which are also capable of removing reactive oxygen species generated by stress [51]. Because of this, after PEG treatment in the transgenic plants many of these compounds reached the same or even lower levels than in the wild type, despite having increased levels in the control condition (Supplementary Table 3). Thus, the low level of several metabolites is likely to be another key factor of the inability of transgenic plants to withstand PEG stress.

3.6 Proposed model for the altered metabolic profile due to NADP-ME2 over-expression during a day-night cycle

The results obtained in this work show that the constitutive over-expression of NADP-ME2 in Arabidopsis leads to an altered metabolite profile, which includes changes not only in organic acids but also in sugars, amino acids and redox compounds (Figures 2 and 3; Table 2), and that affects phenotypic features and stress response (Figures 1 and 4; Table 3). Moreover, NADP-ME2 over-expression alters nocturnal and diurnal cellular processes differentially.

A correlation between NAD(P)/NAD(P)H ratios (Figures 2d and 2e), and the activities and/or transcript levels of ME and MDH (Figure 2; Table 1) at the end of the day and night is very difficult to accomplish given the reversibility of the reactions catalyzed by NADP-ME and MDH. Moreover, these are not the only enzymes that generate or consume NAD(P)(H), e.g. NADPH is produced during the day as a consequence of the photosynthetic process. Nevertheless, taking into account metabolite and pyridine nucleotide pool sizes, enzymatic activities and other parameters we postulate a schematic model of the altered metabolic state observed in NADP-ME2 over-expressing plants during the day and night (Figure 5).

Arabidopsis NADP-ME2 is involved in malate and pyruvate interconversion, with unique reversible properties among other NADP-ME characterized [15,20,52]. In this regard, the transgenic plants show altered malate/pyruvate ratios (Figure 3). The transgenic plants display higher malate and lower pyruvate levels than wild type during both day and night (Figure 3). This fact suggests that NADP-ME2 may be preferentially catalyzing the reductive carboxylation of pyruvate over the malate oxidative decarboxylation in vivo in the transgenic plants (Figure 5).

Apart from modifying malate and pyruvate levels, NADP-ME interconverts NADP and NADPH. In contrast to malate/pyruvate ratio, NADP/NADPH ratio is differentially altered when comparing day versus night in the transgenic plants (Figure 2). At night, both malate/pyruvate and NADP/NADPH ratios are in agreement with an increase of NADP-ME activity in the pyruvate reductive carboxylation direction of the reaction (Figure 5). This altered nocturnal metabolic state, which also includes the increase in the NAD/NADH ratio (Figure 2), is possibly responsible for the drastic decrease in transcript levels and activity of several enzymes involved in malate and redox metabolism (Table 1; Figure 2). Besides the higher level of malate, it is also remarkable the increase in glucose, fructose and starch contents in the transgenic plants (Figure 3), probably due to an altered degradation, which may be linked to several anomalous phenotypic characteristics of the transgenic plants, such as lower root length and rosette weight and delayed flowering time (Figure 1) [53,54].

Although the malate/pyruvate ratio also suggests an increase of NADP-ME activity in the pyruvate reductive carboxylation direction during the day (Figure 5), the NADP/NADPH ratio measured is not in line with this hypothesis. However, considering that NADPH is photosynthetically formed during the day, it is likely that the increase of NADP-ME2 activity in the transgenic plants may affect NADPH dissipation processes, such as the malate valve [46], by increasing cytosolic malate levels, rendering higher NADPH levels than wild type (Figure 3). This hypothesis is in line with the lower F_v/F_m values and CO_2 assimilation rates observed for NADP-ME2 over-expressing plants (Figure 1).

NADP-ME2 over-expressing plants showed a metabolic pattern dissimilar to that observed when the maize photosynthetic NADP-ME was expressed in Arabidopsis. Unlike NADP-ME2 lines, plants over-expressing the maize enzyme presented low levels of carbon metabolites in the form of malate and fumarate, which caused an accelerated dark-induced senescence and a pale green phenotype when the

plants grow in short days [6,7]. In addition to this, NADP-ME2 over-expressing plants showed an opposite osmotic stress behavior to that observed in *A. thaliana* over-expressing a rice cytosolic NADP-ME [25,26]. These contrasting observations could be attributed to the reversibility of the reaction carried out by NADP-ME2. Unlike maize and rice enzymes, which are basically decarboxylating proteins [52], *A. thaliana* recombinant NADP-ME2 exhibited a high catalytic efficiency for reductive carboxylation of pyruvate [15], and this activity was regulated by cell metabolites and pH [20]. Thus, our results bring the first support to the hypothesis that both directions of the reaction may occur in vivo, being affected by a fine, flexible and coordinated regulation in response to cell metabolic status and environmental changes. This complexity may provide important clues for plant fitness bioengineering and a new insight in the understanding of the molecular mechanism that support organic acids metabolism in plant cells.

Acknowledgements

MAT, CSA, MFD and MCGW belong to the Researcher Career of National Council of Scientific and Technical Research (CONICET); MBB and CLA are fellows of the same institution. This work has been financially supported by National Agency for Promotion of Science and Technology, CONICET and Deutsche Forschungsgemeinschaft.

References

[1] C. Sweetman, L.G. Deluc, G.R. Cramer, C.M. Ford, K.L. Soole, Regulation of malate metabolism in grape berry and other developing fruits, Phytochemistry 70 (2009) 1329-1344.
[2] A.R. Fernie, E. Martinoia, Malate. Jack of all trades or master of a few?, Phytochemistry 70 (2009) 828-832.
[3] D. Parker, M. Beckmann, H. Zubair, D.P. Enot, Z. Caracuel-Rios, D.P. Overy, S. Snowdon, N.J. Talbot, J. Draper, Metabolomic analysis reveals a common pattern of metabolic re-programming during invasion of three host plant species by *Magnaporthe grisea*, Plant J. 59 (2009) 723-737.
[4] M.A. Hurth, S.J. Suh, T. Kretzschmar, T. Geis, M. Bregante, F. Gambale, E. Martinoia, H.E. Neuhaus, Impaired pH homeostasis in Arabidopsis lacking the vacuolar dicarboxylate transporter and analysis of carboxylic acid transport across the tonoplast, Plant Physiol. 137 (2005) 901-910.
[5] M. Lee, Y. Choi, B. Burla, Y.Y. Kim, B. Jeon, M. Maeshima, JY Yoo, E Martinoia, Y Lee, The ABC transporter AtABCB14 is a malate importer and modulates stomatal response to CO_2, Nat. Cell Biol. 10 (2008) 1217-1223.
[6] H. Fahnenstich, M. Saigo, M. Niessen, M.F. Drincovich, M.I. Zanor, A. Fernie, C.S. Andreo, U.I. Flügge, V.G. Maurino, Low levels of malate and fumarate cause accelerated senescence during extended darkness in *Arabidopsis thaliana* overexpressing maize C_4 NADP-malic enzyme, Plant Physiol. 145 (2007) 640-655.
[7] M.B. Zell, H. Fahnenstich, A. Maier, M. Saigo, E.V. Voznesenskaya, G.E. Edwards, C.S. Andreo, F. Schleifenbaum, C. Zell, M.F. Drincovich, V.G. Maurino, Analysis of *A. thaliana* with highly reduced levels of malate and fumarate sheds light on the role of these organic acids as storage carbon molecules, Plant Physiol. 152 (2010) 1251-1262.
[8] I. Finkemeier, A.C. König, W. Heard, A. Nunes-Nesi, P.A. Pham, D. Leister, A.R. Fernie, L.J. Sweetlove, Transcriptomic analysis of the role of carboxylic acids in metabolite signalling in Arabidopsis leaves, Plant Physiol. 162 (2013) 239-253.
[9] M.F. Drincovich, M.V. Lara, V.G. Maurino, C.S. Andreo, C_4 decarboxylases: different solutions for the same biochemical problem, the provision of CO_2 to Rubisco in the bundle sheath cells, in: A.S. Raghavendra, R.F. Sage (Eds.), C_4 photosynthesis and related CO_2 concentrating mechanisms, Springer Netherlands, Heidelberg, 2011, 277-300.
[10] D.W. Chia, T.J. Yoder, W.D. Reiter, S.I. Gibson, Fumaric acid: an overlooked form of fixed carbon in Arabidopsis and other plant species. Planta 211 (2000) 743-751.
[11] W.L. Araújo, A. Nunes-Nesi, A.R. Fernie, Fumarate: multiple functions of a simple metabolite. Phytochemistry 72 (2011) 838-843.
[12] M.C. Gerrard Wheeler, M.A. Tronconi, M.F. Drincovich, C.S. Andreo, U.I. Flügge, V.G. Maurino, A comprehensive analysis of the NADP-malic enzyme gene family of *Arabidopsis thaliana*, Plant Physiol. 139 (2005) 39-51.
[13] M.A. Tronconi, H. Fahnenstich, M.C. Gerrard Wheeler, C.S. Andreo, U.I. Flügge, M.F. Drincovich, V.G. Maurino, Arabidopsis NAD-malic enzyme functions as a homodimer and heterodimer and has a major impact during nocturnal metabolism, Plant Physiol. 146 (2008) 1540-1552.
[14] M.C. Gerrard Wheeler, C.L. Arias, V.G. Maurino, C.S. Andreo, M.F. Drincovich, Identification of domains involved in the allosteric regulation of cytosolic *Arabidopsis thaliana* NADP-malic enzymes, FEBS J. 276 (2009) 5665-5677.
[15] M.C. Gerrard Wheeler, C.L. Arias, M.A. Tronconi, V.G. Maurino, C.S. Andreo, M.F. Drincovich, *Arabidopsis thaliana* NADP-malic enzyme isoforms: high degree of identity but clearly distinct properties, Plant Mol. Biol. 67 (2008) 231-242.
[16] M.A. Tronconi, V.G. Maurino, C.S. Andreo, M.F. Drincovich, Three different and tissue-specific NAD-malic enzyme generated by alternative subunit association in *Arabidopsis thaliana*, J. Biol. Chem. 285 (2010) 11870-11879.
[17] M.A. Tronconi, M.C. Gerrard Wheeler, V.G. Maurino, M.F. Drincovich, C.S. Andreo (2010), NAD-malic enzymes of *Arabidopsis thaliana* display distinct kinetic mechanisms that support differences in physiological control, Biochem. J. 430 (2010) 295-303.
[18] M.A. Tronconi, M.C. Gerrard Wheeler, M.F. Drincovich, C.S. Andreo, Diferential fumarate binding to Arabidopsis NAD^+-malic enzymes 1 and -2 produces an opposite activity modulation, Biochimie 94 (2012) 1421-1430.
[19] M.A. Tronconi, M.C. Gerrard Wheeler, A. Martinatto, J.P. Zubimendi, C.S. Andreo, M.F. Drincovich, Allosteric substrate inhibition of Arabidopsis NAD-dependent malic enzyme 1 is released by fumarate, Phytochemistry 111 (2015) 37-47.
[20] C.L. Arias, C.S. Andreo, M.F. Drincovich, M.C. Gerrard Wheeler, Fumarate and cytosolic pH as modulators of the synthesis or consumption of C_4 organic acids through NADP-malic enzyme in *Arabidopsis thaliana*, Plant Mol. Biol. 81 (2013) 297-307.

[21] V.G. Maurino, M.C. Gerrard Wheeler, C.S. Andreo, M.F. Drincovich, Redundancy is sometimes seen only by the uncritical: does Arabidopsis need six malic enzyme isoforms?, Plant Sci. 176 (2009) 715-721.
[22] N.J. Brown, B.G. Palmer, S. Stanley, H. Hajaji, S.H. Janacek, H.M. Astley, K. Parsley, K. Kajala, W.P. Quick, S. Trenkamp, A.R. Fernie, V.G. Maurino, J.M. Hibberd, C_4 acid decarboxylases required for C_4 photosynthesis are active in the mid-vein of the C_3 species *Arabidopsis thaliana*, and are important in sugar and amino acid metabolism, Plant J. 61 (2010) 122-133.
[23] L.M. Voll, M.B. Zell, T. Engelsdorf, A. Saur, M.C. Gerrard Wheeler, M.F. Drincovich, A.P.M. Weber, V.G. Maurino, Loss of cytosolic NADP-malic enzyme 2 in Arabidopsis is associated with enhanced susceptibility towards *Colletotrichum higginsianum*, New Phytol. 195 (2012) 189-202.
[24] S. Li, A. Mhamdi, C. Clement, Y. Jolivet, G. Noctor, Analysis of knockout mutants suggests that Arabidopsis NADP-malic enzyme 2 does not play an essential role in responses to oxidative stress of intracellular or extracellular origin, J. Exp. Bot. 64 (2013) 3605-3614.
[25] S. Liu, Y. Cheng, X. Zhang, Q. Guan, S. Nishiuchi, K. Hase, T. Takano, Expression of an NADP-malic enzyme gene in rice (*Oryza sativa*. L) is induced by environmental stresses; over-expression of the gene in Arabidopsis confers salt and osmotic stress tolerance, Plant Mol. Biol. 64 (2007) 49-58.
[26] Y. Chen, M. Long, A cytosolic NADP-malic enzyme gene from rice (*Oryza sativa* L.) confers salt tolerance in transgenic Arabidopsis, Biotechnol. Lett. 29 (2007) 1129-1134.
[27] T. Murashige, F. Skoog, A revised medium for rapid growth and bioassays with tobacco tissue cultures, Physiol. Plant. 15 (1962) 473-497.
[28] J.F.G.M. Wintermans, A. De Mots, Spectrophotometric characteristics of chlorophylls a and b and their pheophytins in ethanol, Biochim. Biophys. Acta 109(1965) 448-453.
[29] K. Yoshida, I. Terashima, K. Noguchi, Up-regulation of mitochondrial alternative oxidase concomitant with chloroplast over-reduction by excess light. Plant Cell Physiol. 48 (2007) 606-614.
[30] M.W. Pfaffl, A new mathematical model for relative quantification in real-time RT-PCR, Nucleic Acids Res. 29 (2001) e45.
[31] T. Czechowski, M. Stitt, T. Altmann, M.K. Udvardi, W.R. Scheible, Genome-wide identification and testing of superior reference genes for transcript normalization in Arabidopsis, Plant Physiol. 139 (2005) 5-17.
[32] W. Liu, D.A. Saint, A new quantitative method of real time reverse transcription polymerase chain reaction assay based on simulation of polymerase chain reaction kinetics, Anal. Biochem. 302 (2002) 52-59.
[33] J. Hellemans, G. Mortier, A. De Paepe, F. Speleman, J. Vandesompele, qBase relative quantification framework and software for management and automated analysis of real-time quantitative PCR data, Genome Biol. 8 (2007) R19.
[34] G. Queval, G. Noctor, A plate reader method for the measurement of NAD, NADP, glutathione, and ascorbate in tissue extracts: Application to redox profiling during Arabidopsis rosette development, Anal. Biochem. 363 (2007) 58-69.
[35] H. Thordal-Christensen, Z. Zhang, Y. Wei, D.B. Collinge, Subcellular localization of H_2O_2 in plants. H_2O_2 accumulation in papillae and hypersensitive response during the barley-powdery mildew interaction, Plant J. 11 (1997) 1187-1194.
[36] M. Stitt, R.M.C. Lilley, R. Gerhardt, H.W. Heldt, Determination of metabolite levels in specific cells and subcellular compartments of plant leaves, Methods Enzymol. 174 (1989) 518-522.
[37] H.U. Bergmeyer, Methods of enzymatic analysis, second ed., Academic Press Inc., New York and London, 1974.
[38] J. Lisec, N. Schauer, J. Kopka, L. Willmitzer, A.R. Fernie, Gas chromatography mass spectrometry-based metabolite profiling in plants, Nat. Protoc. 1 (2006) 387-396.
[39] J. Kopka, N. Schauer, S. Krueger, C. Birkemeyer, B. Usadel, E. Bergmüller, P. Dörmann, W. Weckwerth, Y. Gibon, M. Stitt, L. Willmitzer, A.R. Fernie, D. Steinhauser, GMD@CSB.DB: the Golm Metabolome Database, Bioinformatics 21 (2005) 1635-1638.
[40] C.E. Alvarez, E. Detarsio, S. Moreno, C.S. Andreo, M.F. Drincovich, Functional characterization of residues involved in redox modulation of maize photosynthetic NADP-malic enzyme activity, Plant Cell Physiol. 53 (2012) 1144-1153.
[41] Q. Yao, H. Ge, S. Wu, N. Zhang, W. Chen, C. Xu, J. Gao, J.J. Thelen, D. Xu, P^3DB 3.0: From plant phosphorylation sites to protein networks, Nucleic Acids Res. 42 (2014) 1206-1213.
[42] M. Berkemeyer, R. Scheibe, O. Ocheretina, A novel, non-redox-regulated NAD-dependent malate dehydrogenase from chloroplasts of *Arabidopsis thaliana* L, J. Biol. Chem. 273 (1998) 27927-27933.
[43] I. Pracharoenwattana, J.E. Cornah, S.M. Smith, Arabidopsis peroxisomal malate dehydrogenase functions in beta-oxidation but not in the glyoxylate cycle, Plant J. 50 (2007) 381-390.

[44] A.B. Cousins, I. Pracharoenwattana, W. Zhou, S.M. Smith, M.R. Badger, Peroxisomal malate dehydrogenase is not essential for photorespiration in Arabidopsis but its absence causes an increase in the stoichiometry of photorespiratory CO_2 realease, Plant Physiol. 148 (2008) 786-795.
[45] T. Tomaz, M. Bagard, I. Pracharoenwattana, P. Lindén, C.P. Lee, A.J. Carroll, E. Ströher, S.M. Smith, P. Gardeström, A.H. Millar, Mitochondrial malate dehydrogenase lowers leaf respiration and alters photorespiration and plant growth in Arabidopsis, Plant Physiol. 154 (2010) 1143-1157.
[46] I. Hebbelmann, J. Selinski, C. Wehmeyer, T. Goss, I. Voss, P. Mulo, S. Kangasjärvi, E.M. Aro, M.L. Oelze, K.J. Dietz, A. Nunes-Nesi, P.T. Do, A.R. Fernie, S.T. Talla, A.S. Raghavendra, V. Linke, R. Scheibe, Multiple strategies to prevent oxidative stress in Arabidopsis plants lacking the malate valve enzyme NADP-malate dehydrogenase, J. Exp. Bot. 63 (2012) 1445-1459.
[47] S. Beeler, H.C. Liu, M. Stadler, T. Schreier, S. Eicke, W.L. Lue, E. Truernit, S.C. Zeeman, J. Chen, O. Kötting, Plastidial NAD-dependent malate dehydrogenase is critical for embryo development and heterotrophic metabolism en Arabidopsis, Plant Physiol. 164 (2014) 1175-1190.
[48] C.H. Foyer, G. Noctor, Redox regulation in photosynthetic organism: signaling, acclimation, and practical implications, Antioxid. Redox Signal. 11 (2009) 861-905.
[49] B. Muller, F. Pantin, M. Génard, O. Turc, S. Freixes, M. Piques, Y. Gibon, Water deficits uncouple growth from photosynthesis, increase C content, and modify the relationships between C and growth in sink organs, J. Exp. Bot. 62 (2011) 1715-1729.
[50] S. Lehmann, C. Gumy, E. Blatter, S. Boeffel, W. Fricke, D. Rentsch, In planta function of compatible solute transporters of the AtProT family, J. Exp. Bot. 62 (2011) 787-796.
[51] A. Nishizawa, Y. Yabuta, S. Shigeoka, Galactinol and raffinose constitute a novel function to protect plants from oxidative damage, Plant Physiol. 147 (2008) 1251-1263.
[52] M. Saigo, C.E. Alvarez, C.S. Andreo, M.F. Drincovich, Plastidial NADP-malic enzymes from grasses: Unraveling the way to the C_4 specific isoforms, Plant Physiol. Biochem. 63 (2013) 39-48.
[53] A. Tiessen, J.H. Hendriks, M. Stitt, A. Branscheid, Y. Gibon, E.M. Farré, P. Geigenberger, Starch synthesis in potato tubers is regulated by post-translational redox modification of ADP-glucose pyrophosphorylase: a novel regulatory mechanism linking starch synthesis to the sucrose supply, Plant Cell 14 (2002) 2191-2213.
[54] D.C. Centeno, S. Osorio, A. Nunes-Nesi, A.L. Bertolo, R.T. Carneiro, W.L. Araújo, M.C. Steinhauser, J. Michalska, J. Rohrmann, P. Geigenberger, S.N. Oliver, M. Stitt, F. Carrari, JK Rose, AR Fernie, Malate plays a crucial role in starch metabolism, ripening, and soluble solid content of tomato fruit and affects postharvest softening. Plant Cell 23 (2011) 162-184.

Figure Captions

Fig. 1 Phenotypic parameters, pigment and starch content of NADP-ME2 over-expressing plants (a) 21-day-old individuals of the over-expressing lines 7.11, 4.20 and 6.20 compared to wild type (b) Root length of 14-day-old plants. (c) Rosette fresh weight of 32-day-old plants. (d) Appearance time of floral primordial. (e) Number of siliques per plant 18 days after flowering. (f) Number of seeds per plant 18 days after flowering. (g) Percentage of germinated seeds. (h) Chlorophyll a content. (i) Chlorophyll b content. (j) Carotenoid content. (k) CO_2 assimilation of 36-day-old leaves. (l) F_v/F_m of 32-day-old plants. (m) Hydrolyzed glucose from starch in samples collected at the end of the day. FW: fresh weight. The lines on the bars indicate the standard deviation of the parameters measured in 20 plants (b-f), in 3 plates with 100 seeds (g), in 3-6 independent preparations (h-j; m) or determined in 6 plants (k-l). The asterisk (*) indicates significant difference ($p < 0.05$) between the values of wild type and 7.11 plants. Changes in the parameters in line 7.11 compared to wild type plant were also confirmed using lines 4.20 and 6.20 (Supplementary Figure 1).

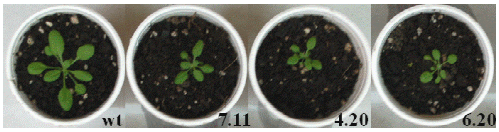

a

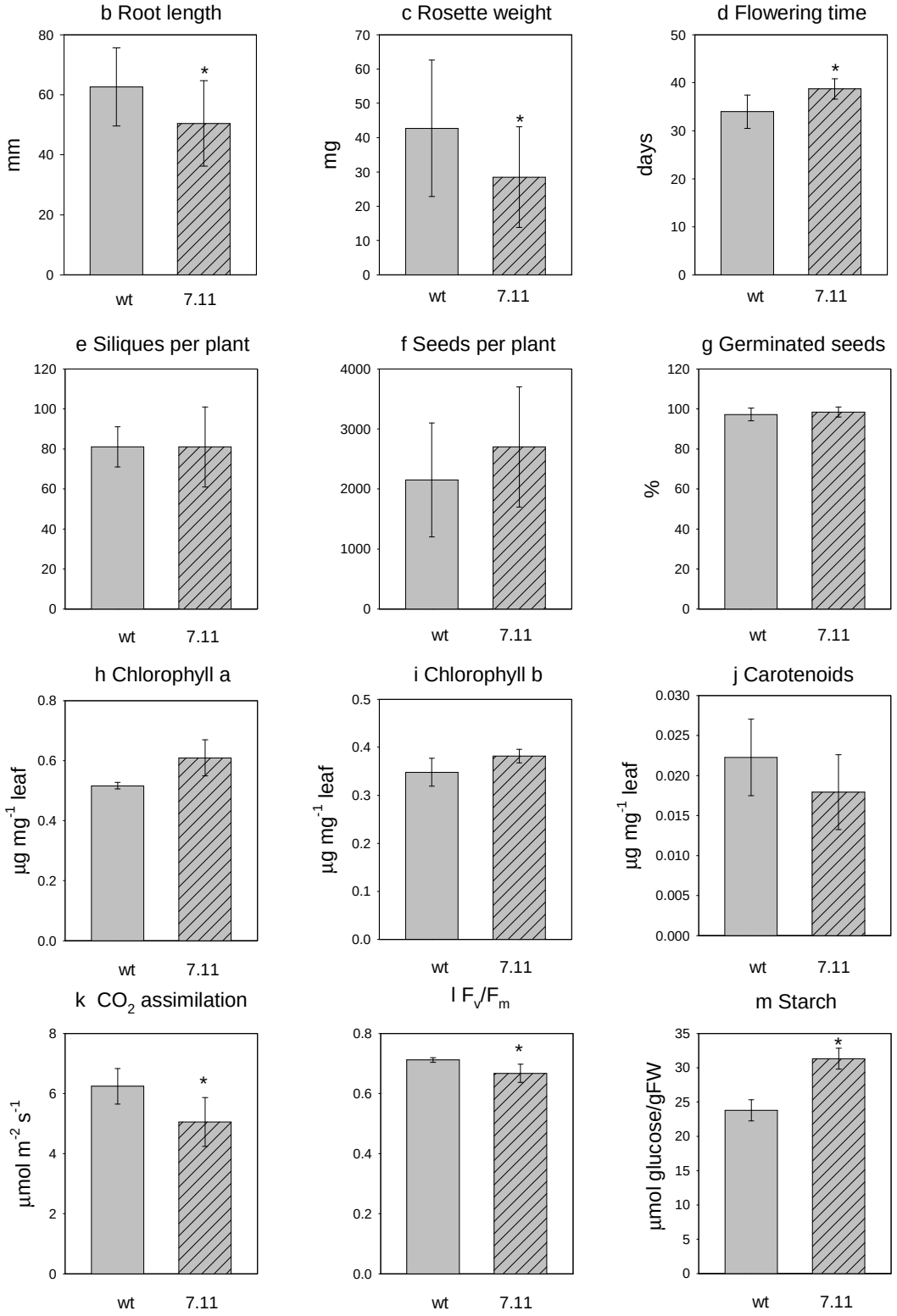

Fig. 2 Enzymatic activities, pyridine nucleotides and H_2O_2 stain in leaves of NADP-ME2 over-expressing plants (a) NADP-ME activity. Native PAGE assayed for NADP-ME activity is shown an inset (50 µg of total protein of each crude extract were loaded). (b) NAD-ME activity. (c) NAD-MDH activity. (d) NADP-MDH initial (i) and total (t) activity before and after incubating each protein extract with 100 mM DTT (e) NADP/NADPH ratio. (f) NAD/NADH ratio. NAD(P)(H) contents were determined using calibration curves. Decrease (↓), increase (↑) or equal levels (=) detected in 7.11 relative to wild type are indicated. Determinations were performed in 6-10 extracts from wt or 7.11 plant samples taken 30 minutes before the end of the day (D) or night (N). The asterisk (*) indicates significant difference ($p < 0.05$) comparing the values of wild type and 7.11 plants. (g) DAB stain of wild type and 7.11 leaves collected in the middle of the light cycle.

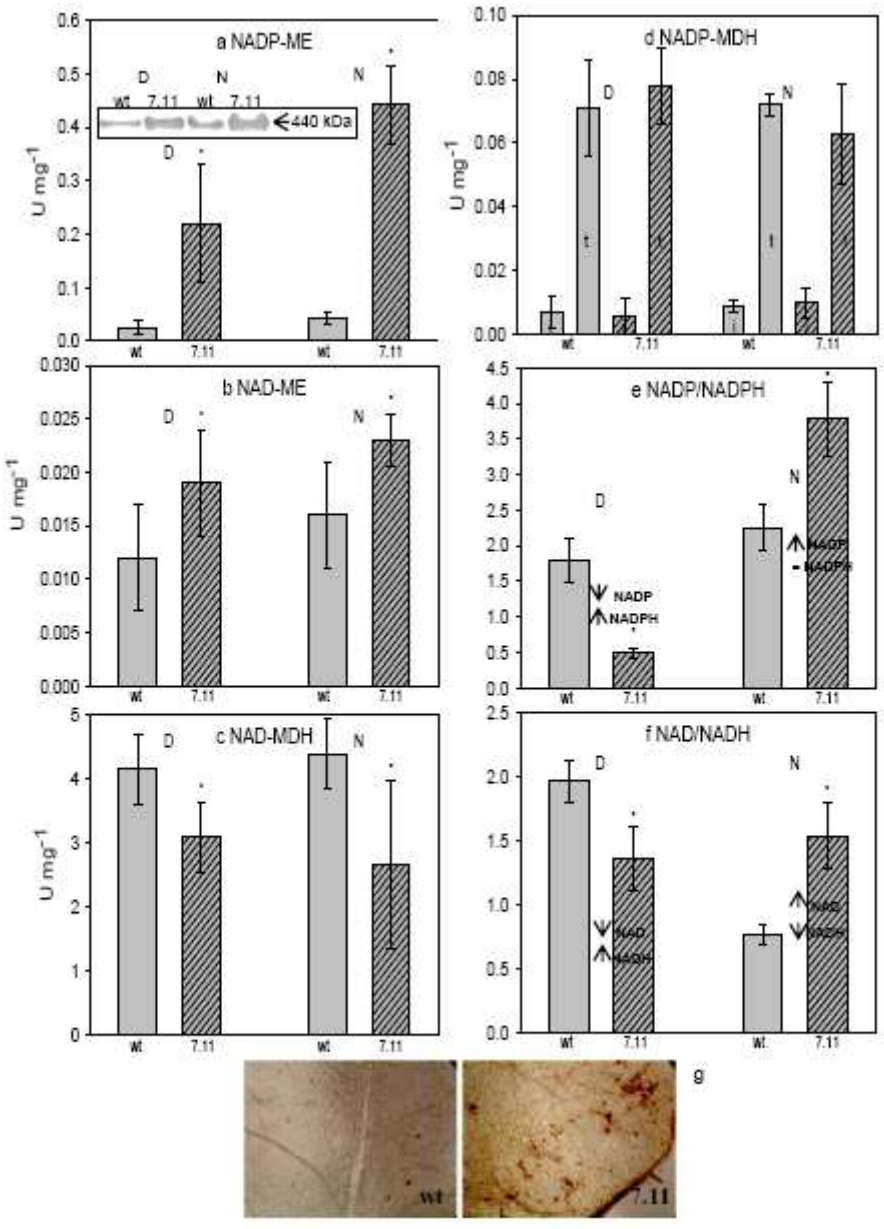

Fig. 3 Level of polar metabolites in rosette leaves of NADP-ME2 over-expressing plants Enzymatic determination of malate, fumarate, pyruvate, glucose, fructose and sucrose content of 7.11 and wild type complete rosettes under normal growth conditions. The moles of each compound were determined using calibration curves. FW: fresh weight. Determinations were performed in extracts from wt or 7.11 plant samples taken 30 minutes before the end of the day (D) or night (N). The lines on the bars indicate the standard deviation of 6-10 preparations. The asterisk (*) indicates significant difference ($p < 0.05$) between the values of wild type and 7.11 plants.

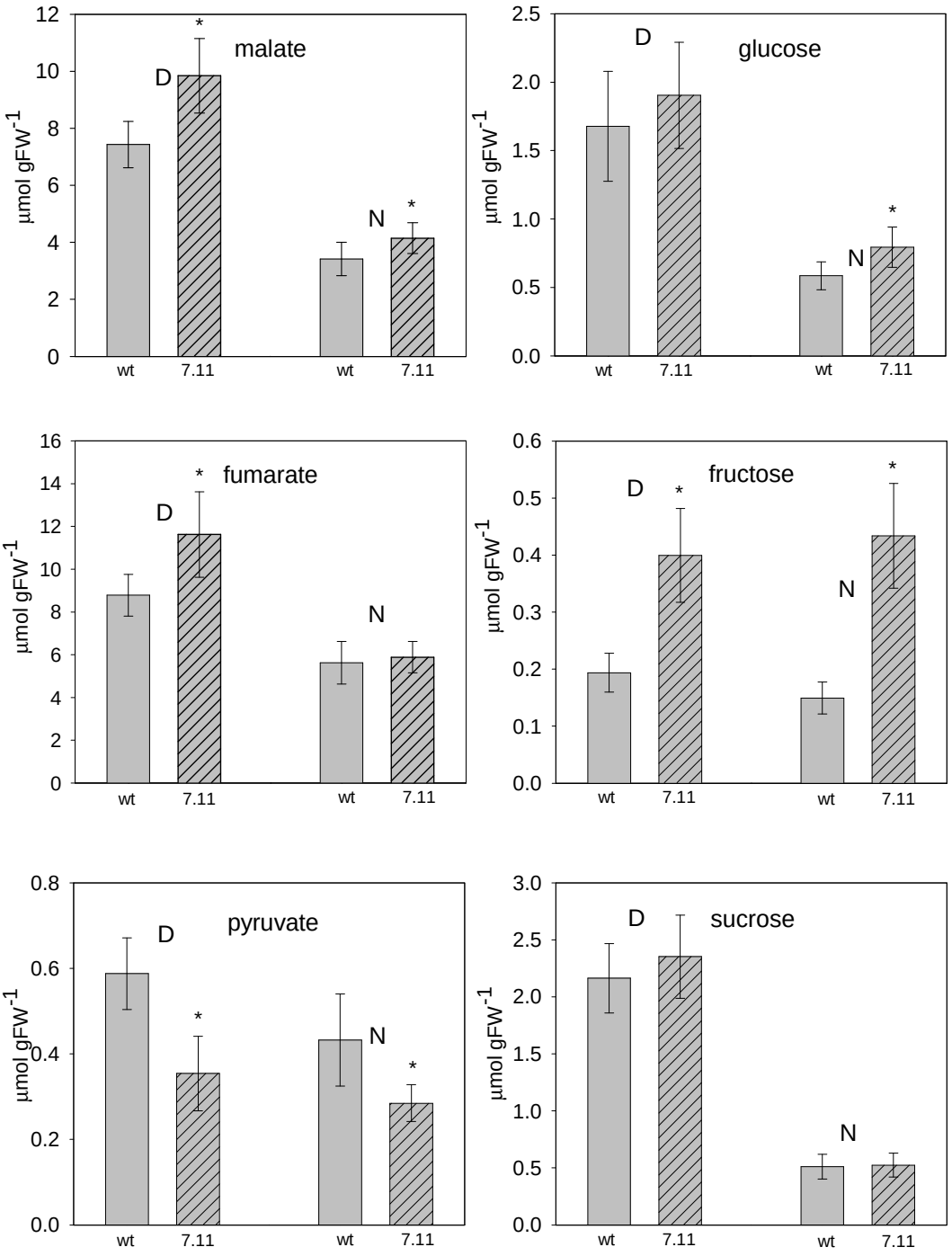

Fig. 4 Differential stress response of NADP-ME2 over-expressing plants (a) NADP-ME2 transgenic 7.11, 4.20 and 6.20 and wild type plants after 14 days of PEG treatment. (b) Percentage of damaged plants after NaCl, PEG or drought treatments. The extent of the stress damage was determined by visual examination and according to rosette appearance. We considered stress damaged plants those showing chlorosis in 75-100% of their leaves. The standard deviation of 4 independent experiments with a total of 16 plants per line in each is indicated (c) Percentage of germinated seeds. The standard deviation using 3 plates with 100 seeds in each is indicated. (d) Pyridine nucleotide contents in PEG-treated samples relative to untreated ones. (e) Polar metabolite contents in PEG-treated samples relative to untreated ones. The determinations in (d) and (e) were performed using enzymatic methods. The ratio between the average values of 6-10 preparations for each sample type, PEG-treated and control plants, is shown. The asterisk (*) indicates significant difference ($p < 0.05$) comparing the values of wild type and 7.11 plants. The horizontal lines represent the point where there is no difference between PEG and control contents (PEG/control = 1).

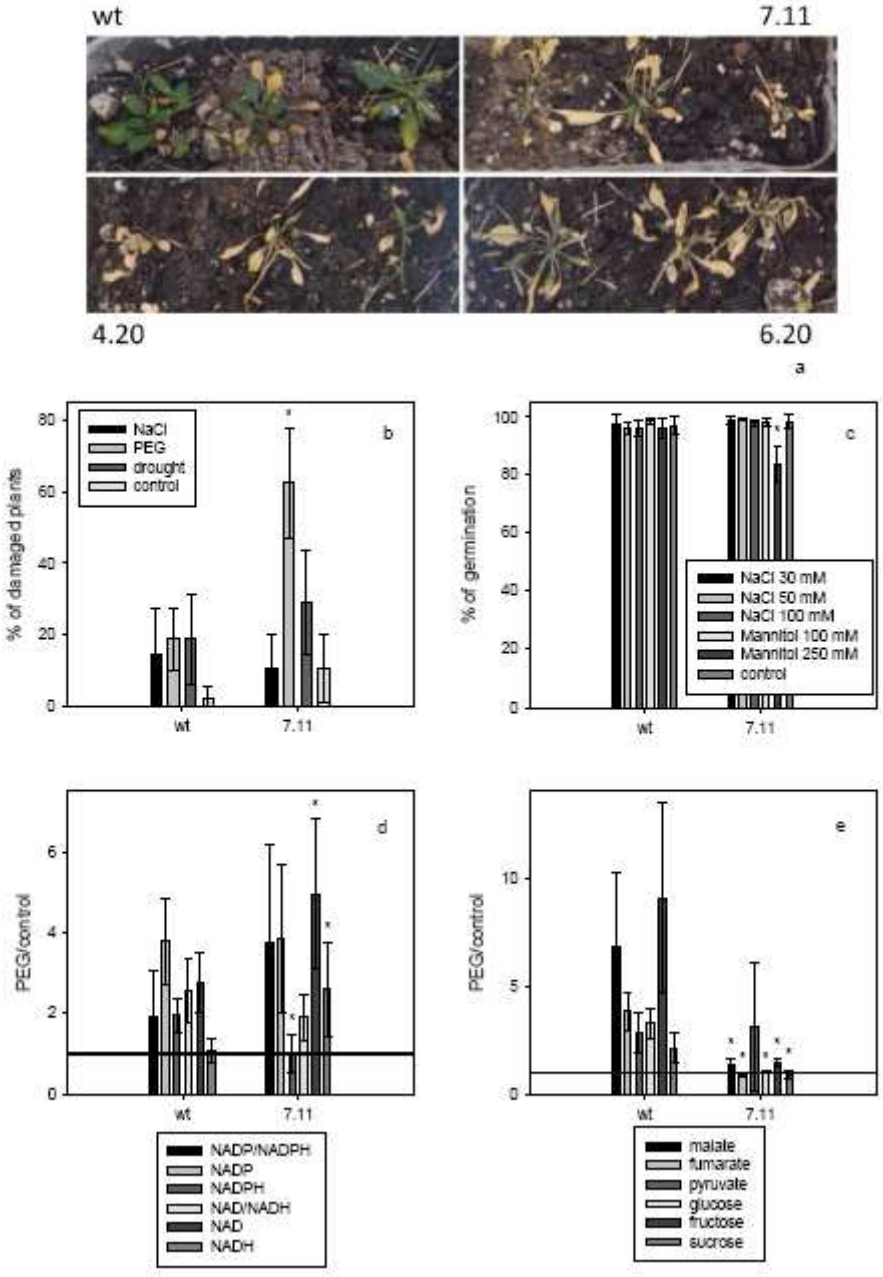

Fig. 5 Schematic representation of the altered metabolic state observed in the NADP-ME2 over-expressing plants during the day and night The arrows denote the increase or decrease in metabolite, enzyme or parameter regarding to the wild type plant. According to the levels of malate, pyruvate, NADP and NADPH, NADP-ME2 may be preferentially catalyzing the reductive carboxylation of pyruvate over the malate oxidative decarboxylation in the transgenic plants during both day and night. At day, NADPH is also formed by photosynthesis, so the NADP/NADPH ratio measured does not strictly reflect this direction of the reaction. The increase of NADP-ME2 activity may affect NADPH dissipation processes decreasing the photosynthetic performance of the transgenic plant. At night, the altered metabolic state includes the increase in the NAD/NADH ratio, possibly causing the decrease in the transcript level and activity of several MDH isoforms. In addition, the higher glucose, fructose and starch contents in the transgenic plants, probably due to an altered degradation, may be linked to the anomalous phenotype of the transgenic plants.

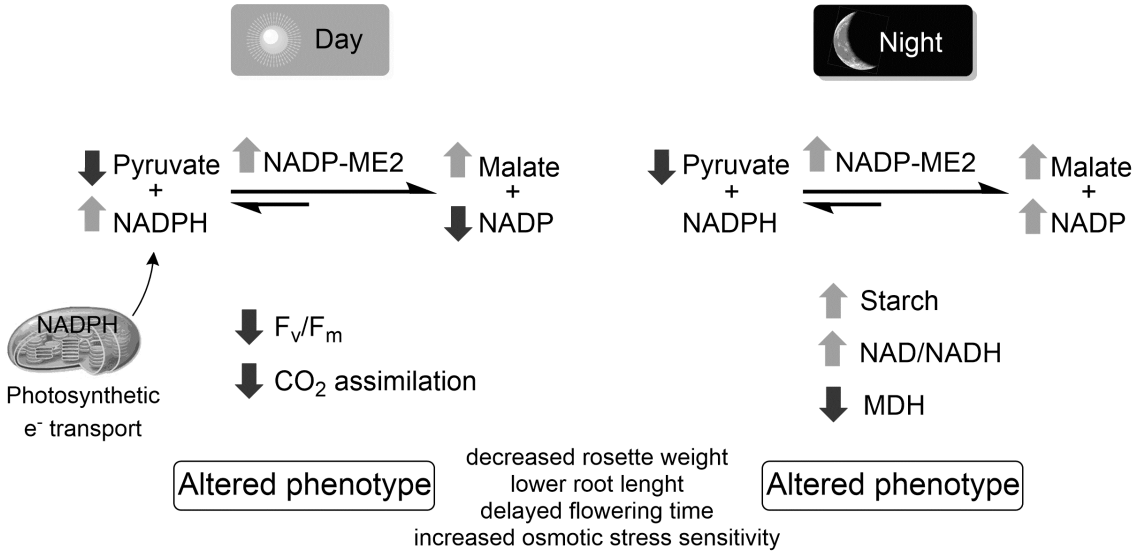

Tables

Table 1 Expression level of the transcripts of NAD(P)-ME and MDH isoforms in leaves of *Arabidopsis thaliana* 7.11 over-expressing line relative to wild type *cyt* (cytosol), *mt* (mitochondria), *px* (peroxisome) and *pt* (plastid) denotes predicted or experimentally confirmed subcellular localization of the encoded proteins. The values are the average of the ratios obtained in at least two independent experiments ± SD. Significant increase or decrease ($p < 0.05$) is indicated in bold type.

	End of the day	End of the night
cyt nadp-me2 (At5g11670)	**22 ± 3**	**27 ± 1**
*pt nadp-me4 (*At1g79750)	1.1 ± 0.5	**0.2 ± 0.1**
mt nad-me1 (At2g13560)	**2.2 ± 0.1**	**0.06 ± 0.01**
mt nad-me2 (At4g00570)	1.0 ± 0.4	**0.3 ± 0.1**
cyt nad-mdh1 (At1g04410)	0.9 ± 0.2	1.1 ± 0.2
cyt nad-mdh2 (At5g43330)	0.8 ± 0.1	**0.52 ± 0.05**
cyt nad-mdh3 (At5g56720)	0.7 ± 0.2	**0.29 ± 0.05**
mt nad-mdh1 (At1g53240)	1.1 ± 0.2	0.76 ± 0.04
mt nad-mdh2 (At3g15020)	1.1 ± 0.2	0.72 ± 0.04
px nad-mdh1 (At2g22780)	1.3 ± 0.2	**0.32 ± 0.02**
px nad-mdh2 (At5g09660)	0.88 ± 0.01	**0.6 ± 0.1**
pt nad-mdh (At3g47520)	1.30 ± 0.03	**0.6 ± 0.2**
pt nadp-mdh (At5g58330)	1.0 ± 0.1	**0.64 ± 0.02**

Table 2 Rosette leaves metabolite contents of line 7.11 relative to wild type determined by GC-MS in normal growth conditions The values are the ratios of each metabolite average obtained in three independent experiments ± SD. Significant increase or decrease ($p < 0.05$) is indicated in bold type. The entire data set of metabolite levels relative to the internal standard ribitol is available in Supplementary Table 2.

7.11/wt	End of the day	End of the night
Alanine	0.8 ± 0.1	**1.6 ± 0.1**
Citrate	**3.0 ± 0.8**	0.7 ± 0.3
G3P	**5.4 ± 2.5**	**2.6 ± 0.5**
GABA	1.2 ± 0.2	1.0 ± 0.2
Galactinol	1.3 ± 0.1	**3.0 ± 1.3**
Galactitol	1.2 ± 0.2	0.8 ± 0.3
Galactose	0.6 ± 0.1	1.1 ± 0.1
Glutamate	0.6 ± 0.1	1.4 ± 0.2
Glycerate	0.9 ± 0.4	1.0 ± 0.1
Glycerol	0.9 ± 0.3	0.6 ± 0.3
Glycine	0.8 ± 0.4	**2.0 ± 0.4**
Lactate	1.1 ± 0.5	**2.8 ± 0.4**
Maleate	**1.6 ± 0.3**	**1.6 ± 0.6**
Maltose	**6.2 ± 2.6**	**2.4 ± 0.7**
myo-inositol	1.0 ± 0.4	0.9 ± 0.4
Oxalate	**3.2 ± 0.8**	**2.1 ± 0.6**
Phosphate	0.8 ± 0.3	**0.2 ± 0.1**
Serine	0.6 ± 0.1	**1.5 ± 0.4**
Succinate	**1.9 ± 0.7**	**0.5 ± 0.2**
Threonine	0.6 ± 0.1	**1.7 ± 0.7**
Trehalose	**0.4 ± 0.1**	**2.7 ± 0.3**
Urea	1.2 ± 0.1	**2.1 ± 0.4**
Valine	0.6 ± 0.3	**2.5 ± 1.0**

Table 3 Metabolite contents determined by GC-MS of wild type and 7.11 PEG-treated plants relative to untreated ones (control) The values are the ratios of each metabolite average obtained in three independent experiments ± SD. Significant increase or decrease ($p < 0.05$) is indicated in bold type.

PEG/control	wt	7.11
Alanine	**9.7 ± 1.5**	**1.8 ± 0.1**
Aspartate	**2.6 ± 0.5**	**2.1 ± 0.4**
Citrate	**2.6 ± 0.4**	**8.3 ± 2.4**
G3P	**1.8 ± 0.2**	**4.4 ± 0.5**
GABA	**5.6 ± 2.3**	**2.7 ± 0.7**
Galactinol	**2.9 ± 0.3**	**0.4 ± 0.1**
Galactitol	**3.1 ± 0.8**	**0.5 ± 0.2**
Galactose	**3.4 ± 0.1**	0.9 ± 0.1
Glutamate	**2.6 ± 0.2**	**2.4 ± 0.2**
Glycerate	**3.0 ± 0.9**	1.4 ± 0.3
Glycerol	**2.1 ± 0.8**	**3.4 ± 0.2**
Glycine	**4.2 ± 1.3**	**1.8 ± 0.2**
Glycolate	**3.9 ± 1.6**	0.7 ± 0.3
Homocysteine	**2.1 ± 0.6**	**1.6 ± 0.3**
Lactate	**1.7 ± 0.8**	1.2 ± 0.4
Maleate	**2.0 ± 0.3**	**1.7 ± 0.6**
Malonate	**2.7 ± 0.6**	**1.7 ± 0.2**
Maltose	1.2 ± 0.1	1.1 ± 0.5
Melibiose	**10.0 ± 3.0**	**0.1 ± 0.1**
myo-inositol	**2.9 ± 0.2**	0.6 ± 0.3
Oxalate	0.9 ± 0.4	**2.7 ± 0.6**
Phosphate	**3.2 ± 0.8**	**2.8 ± 0.5**
Pinitol	**2.3 ± 0.9**	**3.9 ± 0.2**
Raffinose	**5.8 ± 2.7**	**0.2 ± 0.1**
Serine	**2.1 ± 0.2**	**0.5 ± 0.2**
Shikimate	1.2 ± 0.1	**1.7 ± 0.2**
Succinate	**3.6 ± 1.5**	1.3 ± 0.2
Threonine	**2.4 ± 0.8**	0.6 ± 0.2
Trehalose	0.7 ± 0.3	**2.0 ± 0.8**
Urea	**1.8 ± 0.9**	**3.4 ± 0.3**
Valine	**9.0 ± 2.2**	0.8 ± 1.0